Autophagy is required for self-incompatible pollen rejection in two transgenic *Arabidopsis thaliana* accessions

Stuart R. Macgregor,[a,1] Hyun Kyung Lee,[a,1] Hayley Nelles,[a] Daniel C. Johnson,[a] Tong Zhang,[b] Chaozhi Ma,[b] and Daphne R. Goring[a,c,2,3]

[a]Department of Cell & Systems Biology, University of Toronto, Toronto, Canada M5S 3B2.
[b]National Key Laboratory of Crop Genetic Improvement, National Center of Rapeseed Improvement in Wuhan, Huazhong Agricultural University, Wuhan 430070, China.
[c]Centre for the Analysis of Genome Evolution & Function, University of Toronto, Toronto, Canada M5S 3B2.

[1]These authors contributed equally to the article.

[2]Author for Contact, [3]Senior author: Daphne Goring d.goring@utoronto.ca

Short Title: Autophagy in *Arabidopsis* self-incompatibility

One Sentence Summary: In self-incompatible transgenic *Arabidopsis thaliana* lines, autophagy is an integral part of the cellular responses in the stigma to efficiently block fertilization by self-incompatible pollen.

Author Contributions: DRG conceived the project; DRG, SRM, HKL, HN, DCJ and TZ designed the experiments and analyzed the data; SRM, HKL, HN, DCJ and TZ performed the experiments, DRG and CM supervised the experiments; SRM, HKL, and DRG wrote the manuscript; All authors commented on the manuscript before submission; DRG agrees to serve as the author responsible for contact and ensures communication.

Funding information: This research was supported by a grant from Natural Sciences and Engineering Research Council of Canada to DRG, and HKL was supported by an Ontario Graduate Scholarship.

Abstract

Successful reproduction in the Brassicaceae is mediated by a complex series of interactions between the pollen and the pistil, and some species have an additional layer of regulation with the self-incompatibility trait. While the initial activation of the self-incompatibility pathway by the pollen S-locus protein11/*S*-locus cysteine-rich peptide and the stigma *S* Receptor Kinase is well characterized, the downstream mechanisms causing self-pollen rejection are still not fully understood. In previous studies, we had detected the presence of autophagic bodies with self-incompatible pollinations in *Arabidopsis lyrata* and transgenic *A. thaliana* lines, but it was not known if autophagy was essential for self-pollen rejection. Here, we investigated the requirement of autophagy in this response by crossing mutations in the essential *AUTOPHAGY7* (*ATG7*) gene into two different transgenic self-incompatible *A. thaliana* lines in the Col-0 and C24 accessions. By using these previously characterized transgenic lines that express *A. lyrata* and *A. halleri* self-incompatibility genes, we demonstrated that disrupting autophagy can weaken their self-incompatible responses in the stigma. When the *atg7* mutation was present, an increased number of self-incompatible pollen were found to hydrate and form pollen tubes that successfully fertilized the self-incompatible pistils. Additionally, we confirmed the presence of GFP-ATG8a labelled autophagosomes in the stigmatic papillae following self-incompatible pollinations. Together, these findings support the requirement of autophagy in the self-incompatibility response and add to the growing understanding of the cellular events that take place in the stigma to reject self-pollen.

Key words

Autophagy, self-incompatibility, pollen-pistil interactions, reproduction, *SP11/SCR*, *SRK*, *ARC1*, *ATG7*

Introduction

Reproduction in the Brassicaceae is a tightly controlled process, with many components contributing to successful pollen-pistil interactions (reviewed in Doucet et al., 2016; Mizuta and Higashiyama, 2018; Johnson et al., 2019; Adhikari et al., 2020). The Brassicaceae dry stigma lacks surface secretions and instead regulates the delivery of resources to the pollen shortly after pollination. This leads to the selective hydration of compatible pollen grains, followed by the penetration of the pollen tube into the stigmatic barrier to grow down the reproductive tract (reviewed in Dickinson, 1995; Palanivelu and Tsukamoto, 2012; Doucet et al., 2016; Adhikari et al., 2020). It is also at this initial cell-cell communication stage that self-incompatible pollen is recognized and blocked by the stigma to prevent inbreeding (reviewed in Jany et al., 2019; Nasrallah, 2019; Durand et al., 2020). A recent live-cell imaging study in *Arabidopsis thaliana* compared pollen hydration rates of compatible and self-incompatible pollen grains and found that while compatible pollen grains rapidly hydrated, self-incompatible pollen failed to fully hydrate which then led to a failure in pollen germination or a failure of pollen tubes to penetrate the stigmatic papilla cell wall (Rozier et al., 2020). Furthermore, actin foci were present in the stigmatic papillae at the site of emerging pollen tubes for compatible pollen only. The actin focalization is likely associated with the stigmatic papilla cellular responses to enable compatible pollen hydration and pollen tube penetration (Rozier et al., 2020).

The Brassicaceae self-incompatible response is initiated by the binding of the *S*-haplotype-specific pollen ligand, *S*-locus protein 11/*S*-locus cysteine-rich peptide (SP11/SCR) to the corresponding stigma-specific *S* Receptor Kinase (SRK). This leads to the phosphorylation of the SRK kinase domain and activation of the downstream signaling responses, ultimately leading to the rejection of the self-incompatible pollen grain (reviewed in Jany et al., 2019; Nasrallah, 2019). Not all Brassicaceae species possess this trait due to mutations in the key self-incompatibility genes, *SP11/SCR* and *SRK* (reviewed in Durand et al., 2020). For example, the transition of *A. thaliana* to a fully selfing species is associated with mutations in the *SCR* and *SRK* genes (Kusaba et al., 2001; Shimizu et al., 2008; Boggs et al., 2009; Tsuchimatsu et al., 2010; Guo et al., 2011; Tsuchimatsu et al., 2017). In contrast, other family members like *A. lyrata* and *A. halleri* have intact *SCR* and *SRK* genes, which result in a robust self-incompatibility response upon self-pollination (Kusaba et al., 2001; Schierup et al., 2001; Goubet et al., 2012).

A number of studies have reintroduced the self-incompatibility trait back into *A. thaliana* by introducing *A. lyrata* or *A. halleri SP11/SCR* and *SRK* transgenes (Nasrallah et al., 2004; Boggs et al., 2009; Indriolo et al., 2014; Iwano et al., 2015; Zhang et al., 2019; Rozier et al., 2020). However, the success of this approach was accession-dependent; for example, transgenic experiments in *A. thaliana* Col-0 failed to produce self-incompatible plants, whereas experiments using *A. thaliana* C24 were very successful (Nasrallah et al., 2002; Boggs et al., 2009; Iwano et al., 2015; Rozier et al., 2020). The cause of this was linked to inverted repeats within the *A. thaliana SRKA* pseudogene which triggers RNA silencing of the introduced *SRK* transgenes (Fujii et al., 2020). For the Col-0 accession, the inverted repeat was found in a conserved region of the predicted *pseudoSRKA* kinase domain resulting in the silencing of closely related *SRK* transgenes. For the C24 accession, the inverted repeat was found in a more polymorphic region of the predicted *pseudoSRKA* ectodomain and appeared to be less effective at inducing RNA silencing of related *SRK* transgenes (Fujii et al., 2020).

We have found that a strong self-incompatibility response can also be recapitulated in *A. thaliana* Col-0 when the *A. lyrata* or *A. halleri ARC1* transgene was added along with the *A. lyrata* or *A. halleri SP11/SCR* and *SRK* transgenes (Indriolo et al., 2014; Zhang et al., 2019). The ARC1 E3 ubiquitin ligase is proposed to act directly downstream of SRK in the self-incompatibility signaling pathway (Gu et al., 1998; Stone et al., 1999; Stone et al., 2003). A large part of the *ARC1* gene has been deleted in the *A. thaliana* genome, and knockdowns of *ARC1* in self-incompatible *Brassica napus* and *A. lyrata* resulted in a partial breakdown of self-incompatibility (Stone et al., 1999; Indriolo et al., 2012). ARC1 is proposed to target cellular components that are required in the stigma to accept compatible pollen, such as the EXO70A1 exocyst subunit (Samuel et al., 2009) and *Brassica* GLO1 (Sankaranarayanan et al., 2015). Self-incompatible pollinations also induced a strong and rapid cytosolic calcium influx in the stigmatic papillae (Iwano et al., 2015). These combined self-incompatibility responses are proposed to disrupt the secretory activity in the stigmatic papillae which would be required for compatible pollen acceptance (Dickinson, 1995; Elleman and Dickinson, 1996; Samuel et al., 2009; Safavian and Goring, 2013; Safavian et al., 2015; Goring, 2017).

In previous work, we uncovered signs of autophagy activation in *A. lyrata* and *A. thaliana* stigmatic papillae within 10 minutes of self-incompatible pollinations, but not with compatible pollinations (Safavian and Goring, 2013; Indriolo et al., 2014). TEM images revealed structures

resembling autophagic bodies in the vacuoles of stigmatic papilla following self-incompatible pollinations (Safavian and Goring, 2013; Indriolo et al., 2014). In contrast, TEM images of compatible pollinations revealed vesicle-like structures in the stigmatic papillae under the compatible pollen contact site suggestive of secretory activity (Safavian and Goring, 2013; Indriolo et al., 2014). The presence of autophagosomes in *A. lyrata* self-incompatible pollinations was further confirmed using the GFP-ATG8a autophagosome marker (Safavian and Goring, 2013). Although these studies indicated that autophagy was activated following self-incompatible pollinations, it was unclear whether autophagy is essential for the rejection of self-incompatible pollen. Here, we have used two different self-incompatible (SI) transgenic *A. thaliana* lines (in the Col-0 and C24 accessions; Iwano et al., 2014; Zhang et al., 2019) to test the requirement of the autophagy system for self-pollen rejection. When loss-of-function mutants in the *AUTOPHAGY7* (*ATG7*) gene (Chung et al., 2010; Ding et al., 2018) were combined with the SI-Col-0 and SI-C24 lines, we observed a partial breakdown of the self-incompatibility response in both accessions. This indicates that autophagic activity is required for the effective rejection of self-incompatible pollen, and thus, elucidates an additional downstream cellular event in the self-incompatibility pathway.

Results

Generation of self-incompatible *A. thaliana* transgenic lines carrying the *atg7* mutation to disrupt autophagy

To investigate the involvement of autophagy in self-incompatibility, two different transgenic *A. thaliana* SI lines were used to cross with *atg7* autophagy mutants. ATG7 is an essential component in the formation of autophagosomes (reviewed in Ding et al., 2018), and *atg7* mutations lead to a loss of autophagy (Thompson et al., 2005; Chung et al., 2010; Young et al., 2019). The first self-incompatible line is in the Col-0 accession (SI-Col-0) and carries the *A. halleri SCR13*, *SRK13* and *ARC1* transgenes in a single T-DNA (*Ah-SCR13 Ah-SRK13 Ah-ARC1* #2 line; Zhang et al., 2019). The SI-Col-0 was crossed to the previously characterized *atg7-2* mutant in the Col-0 accession (Chung et al., 2010). The F_1 plants from this cross were selfed, and all pollination assays were carried out in the F_2 generation. The second self-incompatible line is in the C24 accession (SI-C24) and carries the *A. lyrata SCRb* and *SRKb* transgenes (SI-C24 #15-1 line; Iwano et al., 2015). As there were no *atg7* mutants available in the C24 accession, CRISPR/Cas9 technology was used to generate additional *atg7* mutants. Deletion of the *ATG7* gene was confirmed through PCR and sequencing of genomic regions flanking gRNA target sites (Supplemental Fig. S1). The *atg7-9* C24 mutant displayed the same overall wild-type plant and flower morphology (Supplemental Fig. S2) as seen for the *atg7-2* Col-0 mutant. Both *atg7* mutants also displayed the shorter life span typically seen in *atg* mutants as a result of early senescence (premature rosette yellowing; Thompson et al., 2005; Avila-Ospina et al., 2014). The C24 *atg7-9* mutant was crossed with the SI-C24 line, and following selfing of the F_1 plants, all pollination assays were carried out in F_2 generation (T4 generation for the *atg7-9* mutation). For both sets of F_2 progeny, genotyping was first carried to identify the transgenic plants carrying the SI transgenes, followed by genotyping for the *atg7* mutation to identify plants that were wild-type, heterozygous or homozygous for the *atg7* mutation.

Disrupting autophagy breaks down the initial self-incompatible response of blocking pollen hydration

To assess the early stages of pollen rejection, the pollen hydration checkpoint was first investigated. Self-incompatible pollen from the parental SI-Col-0 or SI-C24 transgenic lines were used to pollinate pistils from the respective F_2 progeny segregating for the *atg7* mutation,

and pollen hydration assays were carried out by measuring the increase in pollen diameter at 10 min post-pollination (Lee et al., 2020). Positive controls of the SI-Col-0 and SI-C24 pollen placed on compatible wildtype Col-0 and C24 pistils, respectively, resulted in a large increase in diameter as a result of pollen hydration (Fig. 1A, B). In contrast, self-pollen placed on the SI-Col-0 and SI-C24 pistils resulted in very little pollen hydration at 10-minutes post-pollination (Fig. 1A, B). This lack of hydration was consistent between the SI-Col-0 and SI-C24 lines and indicative of the early recognition and rejection of self-incompatible pollen. Importantly, stigmas from the *atg7-2* and *atg7-9* mutants showed normal SI-Col-0 and SI-C24 pollen hydration, respectively, indicating that disruption in the autophagic process did not perturb the compatible post-pollination responses (Fig. 1A, B).

For the F_2 progeny from the SI-Col-0 x *atg7-2* cross, the SI-Col-0 plants homozygous for wildtype *ATG7* showed the same small increase in pollen hydration as the control self-incompatible pollinations at 10 min post-pollination. In contrast, when SI-Col-0 pollen was applied to the SI-Col-0 stigmas that were either heterozygous or homozygous for the *atg7-2* mutation, an increase in pollen hydration was observed, indicating an incomplete rejection of the self-incompatible pollen (Fig. 1A). When a single *atg7-2* allele was present in the SI-Col-0 background (heterozygous for *atg7-2*), the rate of SI-Col-0 pollen hydration significantly increased. A further significant increase for SI-Col-0 pollen hydration was measured on SI-Col-0 stigmas that were homozygous for the *atg7-2* mutation (Fig. 1A). A comparable set of pollen hydration experiments on the F_2 progeny from the SI-C24 x *atg7-9* cross also showed a similar trend (Fig. 1B). SI-C24 stigmas that were wild-type for *ATG7* supported similar small increases in SI-C24 pollen hydration as the control self-incompatible pollinations, and the introduction of the *atg7-9* mutation into this background resulted in increased hydration of the self-incompatible pollen. Interesting for the SI-C24 line, the same significant increase in SI-C24 pollen hydration was seen for stigmas that were either heterozygous or homozygous for the *atg7-9* mutation (Fig. 1B). Thus, for both self-incompatible lines, even the single allelic loss of *ATG7* can impact the rejection of self-incompatible pollen. Together, these results indicate that autophagy is required to fully prevent the hydration of self-incompatible pollen.

Disruption of autophagy increases self-incompatible pollen tube penetration

200 With the observed increase in self-incompatible pollen hydration, the next stage of preventing
201 self-incompatible pollen germination and pollen tube penetration was investigated. To determine
202 if this block was affected by the *atg7* mutation, pollinated pistils were collected at 2- and 24-
203 hours post-pollination and stained with aniline blue to visualize pollen tubes. At 2-hours post-
204 pollination, SI-Col-0 and SI-C24 pollen was completely rejected by the respective self-
205 incompatible pistils, and no pollen tubes were visible (Supplemental Fig. S2 and S3).
206 Surprisingly, pistils from the F_2 *atg7* homozygous mutants in the SI-Col-0 and SI-C24
207 backgrounds displayed similar results with the SI-Col-0 and SI-C24 pollen efficiently rejected
208 (Supplemental Fig. S2 and S3). This suggested that despite an increase in pollen hydration, the
209 next stage in the self-incompatibility response was not affected at 2-hours post-pollination by the
210 absence of autophagy. Although we did not observe any obvious difference at 2-hours post-
211 pollination, we did observe an occasional pollen tube that penetrated the stigma barrier of the SI-
212 Col-0 and SI-C24 *atg7* homozygous mutants.
213 To address whether we could observe a greater number of SI-Col-0 and SI-C24 pollen tubes after
214 a longer period, pollinated pistil samples were then harvested at 24-hours post-pollination. A
215 later time point following pollination is more reflective of the natural pollination process and
216 provides more time for the self-incompatible pollen to germinate and grow into the pistil. Self-
217 pollination of the SI-Col-0 and SI-C24 parental lines resulted in an absence of pollen tubes (Fig.
218 2A and 3A) while pollinations with compatible wild-type pollen led to an abundance of pollen
219 tubes growing in the pistils (Fig. 2B and 3B). The results indicated that the SI-Col-0 and SI-C24
220 were able to fully reject self-incompatible pollen and accept wild-type compatible pollen at 24-
221 hours post-pollination. The SI-Col-0 and SI-C24 pollen also produced numerous pollen tubes
222 when placed on the *atg7* mutant pistils, indicating that the absence of autophagy did not affect
223 these compatible pollinations (Fig. 2C and 3C). The same result was seen for the wild-type
224 pollen grains deposited on SI-Col-0 *atg7-2* and SI-C24 *atg7-9* mutant pistils (Fig. 2D and 3DC).
225 Finally, we examined the impact of the *atg7* mutation on self-incompatibility at 24-hours post-
226 pollination by applying the SI-Col-0 and SI-C24 pollen on their respective F_2 progeny
227 segregating for the *atg7* mutation. When SI-Col-0 *ATG7/atg7-2* and SI-Col-0 *atg7-2/atg7-2*
228 stigmas were pollinated with SI-Col-0 pollen, there was a general increase in the number of
229 pollen grains adhering to the stigma and forming pollen tubes when compared to the SI-Col-0
230 pistils (Fig. 2E-G). The pollinations were repeated for the SI-C24 F_2 plants, and again the SI-C24

ATG7/atg7-9 and SI-C24 *atg7-9/atg7-9* pistils did show some SI-C24 pollen adhering to the stigmatic surface and successfully growing pollen tubes through the pistil while the SI-C24 *ATG7/ATG7* pistils rejected the SI-C24 pollen (Fig. 3E-G). The number of pollen tubes were counted in the SI-Col-0 and SI-C24 pistils that were wild-type or homozygous for the *atg7* mutation, and a significant increase in the number of pollen tubes were counted in the homozygous *atg7* mutants (Fig. 2G and 3G). Thus, the 24-hours post-pollination samples demonstrated that autophagy is required for fully blocking self-incompatible pollen germination and pollen tube growth through the self-incompatible pistil.

Loss of autophagy increases seed set in the self-incompatible lines

With the observation that self-incompatibility is partially lost in the SI-Col-0 *atg7-2* and SI-C24 *atg7-9* mutant pistils and resulting in more pollen tubes growing through the pistil, the impact of this on seed set was assessed. Manual pollinations were carried out using SI-Col-0 and SI-C24 pollen on pistils from the respective parental lines and F_2 progeny segregating for the *atg7* mutation, and 2-week old siliques were harvested for seed counting (Fig. 4). Autophagy mutants have previously been characterized as having a reduced seed set (Phillips et al., 2008; Minina et al., 2018), and this was observed for the *atg7-2* mutant when pollinated with SI-Col-0 pollen. The *atg7-2* mutant produced an average of 42.3 seeds/silique compared to the 50.8 seeds/silique produced by wild-type Col-0 (Fig. 4A and C). As expected, self-pollination of the SI-Col-0 pistils resulted in a very limited seed yield (12.8 seeds/silique), consistent with the rejection of self-incompatible pollen. When the *atg7-2* mutation was present in the SI-Col-0 pistils, there was a significant increase in yield with 25.3 seeds/silique for SI-Col-0 *ATG7/atg7-2* and 27 seeds/silique for SI-Col-0 *atg7-2/atg7-2* (Fig. 4A and C). This indicates that disruptions in autophagy are sufficient to disrupt the self-incompatibility pathway, thus allowing the growth of more pollen tubes through the pistil to initiate fertilization and seed production.

Similar trends in seed yields were also observed in the C24 accession. When pollinated with SI-C24 pollen, the *atg7-9* mutants yielded an average of 35.3 seeds/silique compared to the wild-type C24 pistils yielding an average of 46 seeds/silique (Fig. 4B and D). Self-incompatible pollinations with SI-C24 pistils resulted in a low average of 6.8 seeds/silique as expected. The presence of the *atg7-9* mutation in SI-C24 pistils resulted in significant increases in seed yields

261 with 16.5 seeds/silique for SI-C24 *ATG7/atg7-9* and 17.2 seeds/silique the SI-C24 *atg7-9/atg7-9*
262 indicating that there was an incomplete rejection of self-pollen in these crosses (Fig. 4B and D).
263 Altogether, these results indicate that loss of autophagy results in an increase in the number of
264 pollen tubes that bypass the self-incompatibility response to successfully fertilize ovules in the
265 SI-Col-0 and SI-C24 lines, confirming that autophagy is required for full rejection of self-pollen.
266 One feature that was observed in all these post-pollination assays was that pistils from both the
267 *ATG7/atg7* heterozygotes and *atg7/atg7* homozygotes in the SI-Col-0 and SI-C24 backgrounds
268 displayed similar weakened phenotypes for the self-incompatibility response. This is quite
269 unusual as previous reports only described mutant phenotypes for the *Arabidopsis atg*
270 homozygotes (reviewed in Marshall and Vierstra, 2018; Qi et al., 2020; Su et al., 2020), unless
271 the *ATG* gene functioned in the haploid male gametophyte (Qin et al., 2007). Consequently, we
272 were puzzled as to why the SI *ATG7/atg7* heterozygotes were presenting these altered
273 phenotypes. One potential explanation could be that *ATG7* expression levels in the stigmatic
274 papillae are sufficiently low for the self-incompatibility response to be impacted by the loss of
275 one *atg7* allele. We used a previously published stigmatic papillae RNA-Seq dataset (Gao et al.,
276 2018) to survey expression levels for the different *A. thaliana ATG* genes in the *ATG8-ATG12*
277 conjugation system and found that *ATG7* was expressed at quite low levels in the receptive
278 stigma stage, the stage used for our pollination experiments (Supplemental Fig. S5). The *ATG7*
279 expression levels increased almost 13-fold in the older stigmatic papillae samples, coinciding
280 with the onset of the stigmatic papillar cell death stage where perhaps autophagy is more
281 typically involved (Supplemental Fig. S5; Gao et al., 2018).
282
283 **Autophagosomes are produced following self-pollination in the SI-C24 line**
284 Previously, autophagosomes were detected following self-incompatible pollinations in *A. lyrata*
285 and in the transgenic self-incompatible *A. thaliana* in the Col-0 accession (Safavian and Goring,
286 2013; Indriolo et al., 2014). To confirm that autophagosomes are also formed in the SI-C24 line,
287 the previously established fluorescent marker for autophagosomes, *GFP-ATG8a* (Thompson et
288 al., 2005), was transformed into the SI-C24 background. The SI-C24 GFP-ATG8a stigmatic
289 papillae were manually pollinated with either SI-C24 or wild-type C24 pollen and imaged at 10
290 minutes post-pollination. Following SI-C24 pollination, several GFP punctae were observed in
291 the stigmatic papillae adjacent to the SI-C24 pollen, indicating the presence of GFP-ATG8a-

292 labelled autophagosomes (Fig. 5A). Conversely, no clear punctae were observed when the SI-
293 C24 GFP-ATG8a stigmatic papillae which pollinated with wild-type compatible C24 pollen (Fig.
294 5B). These observations confirmed our previous findings that autophagy is activated in the
295 stigmatic papillae with self-incompatible pollinations, but not with compatible pollinations
296 (Safavian and Goring, 2013; Indriolo and Goring, 2014).
297
298

Discussion

Self-incompatibility plays an important regulatory role in many outcrossing Brassicaceae species where producing inbred progeny would be disadvantageous (Shimizu and Tsuchimatsu, 2015; Durand et al., 2020). Previous studies have uncovered many important steps in the self-incompatibility pathway, but there are still outstanding questions on the cellular mechanisms by which self-pollen is rejected (reviewed in Doucet et al., 2016; Goring, 2017; Jany et al., 2019). In previous studies, we observed the presence of autophagosomes in the cytoplasm and autophagic bodies in the vacuole with self-incompatible pollinations in self-incompatible *A. lyrata* and transgenic self-incompatible *A. thaliana* Col-0 (Safavian and Goring, 2013; Indriolo and Goring, 2014). What was not known, however, was whether autophagy was necessary for self-incompatible pollen rejection. In this study, we addressed this question by crossing autophagy-deficient mutants (*atg7*) into two different transgenic self-incompatible *A. thaliana* lines, and demonstrated that a functioning autophagy system is required in the stigma for the full rejection of self-incompatible pollen. It is important to note that disrupting autophagy did not cause a full loss of self-incompatibility indicating that other cellular responses are required in conjunction with autophagy for self-incompatible pollen rejection. Importantly, this partial breakdown in the stigma was seen for all stages from increased pollen hydration to more pollen tubes growing through pistil to increase seed yields. Additionally, we observed that a single copy of the *atg7* mutant allele was sufficient to cause a measurable breakdown of the self-incompatibility response. Finally, the requirement of autophagy in the rejection of self-incompatible pollen was consistent between the two different *Arabidopsis thaliana* accessions, Col-0 and C24, indicating that the two share a very similar mechanism for self-incompatible pollen rejection.

The rationale for using both the SI-Col-0 and SI-C24 lines was to determine if there were any accession- or transgene-specific associations with autophagy. The SI-Col-0 carries the *A. halleri SCR13*, *SRK13* and *ARC1* transgenes (Zhang et al., 2019) while the SI-C24 line carries the *A. lyrata SCRb* and *SRKb* transgenes (Iwano et al., 2015). In addition to two different S-haplotypes from two different *Arabidopsis* species, the SI-Col-0 line also carries the *A. halleri ARC1* transgene. The fact that both accessions require an intact autophagy system in the stigma for full self-incompatible pollen rejection indicates that autophagy activation does not require ARC1, though the potential involvement of another related PUB E3 ligase cannot be ruled out (Indriolo et al., 2012; Indriolo and Goring, 2016). Our results indicate that autophagy is a clear

commonality in the self-incompatibility response between these two accessions, although variation may exist in the execution of this cellular function. The question then arises to the purpose of autophagy activation in self-incompatibility.

Self-incompatible pollen carries the signals to be recognized as both self-incompatible pollen and compatible pollen, and it has been hypothesized that self-incompatibility blocks compatible pollen responses in the stigma (Dickinson, 1995). With the working model that secretory activity in the stigma is required for compatible pollen acceptance (reviewed in Dickinson, 1995; Doucet et al., 2016; Goring, 2017), several of the self-incompatibility cellular responses such as EX070A1 inhibition (Samuel et al., 2009; Sankaranarayanan et al., 2015), a strong and rapid calcium influx (Iwano et al., 2015), and the absence of actin focalization (Rozier et al., 2020) are consistent with blocking secretion (reviewed in Goring, 2017). Autophagy could also be an additional step to clear any secretory activity that was initially activated. Another possibility is that autophagy is resetting the cellular program to reject self-pollen. (Rodriguez et al., 2020) recently demonstrated a role for autophagy in switching *A. thaliana* cell fate determination following treatments with different signals. Autophagy was shown to be required for this switch and was proposed to "clean-up" the cell to allow for the new cellular program to be established. In the context of self-incompatibility, autophagy activation in the stigma could be linked to reprogramming the cells from the default compatible pollen responses to the self-pollen rejection pathway.

In conclusion, this study now firmly places autophagy as part of the cellular mechanisms leading to self-incompatible pollen rejection. Future studies will need to focus on how autophagy is activated in the self-incompatibility pathway and whether there are specific cytoplasmic components targeted for autophagic destruction. Understanding the mechanisms underlying self-incompatibility is important as seed yield of many important crop species is directly tied to their reproductive success, and the ability to modulate selfing would be a powerful tool in increasing yield.

Materials and methods

Plant materials and growth conditions

All *Arabidopsis thaliana* seeds (Col-0, C24, transgenic lines, T-DNA insertion mutants and CRISPR/Cas9 deletion mutants) were sterilized and cold stratified at 4°C for 3 days. Seedlings

were germinated on ½ Murashige and Skoog (MS) medium plates supplemented with 0.4 (w/v) phytoagar (pH 5.8) and 1% (w/v) sucrose. Seedlings were grown at 22°C under 16h light for 7 days, and then transferred to Sunshine #1 soil supplemented with Plant Prod All Purpose Fertilizer 20-20-20 (1g/L water). All plants were grown in chambers under a 16-hour light/8-hour dark growth cycle at 22°C, with humidity kept under 50%.

For the Col-0 accession experiments, the *Ah-SCR13 Ah-SRK13 Ah-ARC1* #2 Col-0 line (Zhang et al., 2019) was crossed to the *atg7-2* mutant (Col-0 accession; Chung et al., 2010). For the C24 accession experiments, the *SI-C24 #15-1* line (with *Al-SCRb AlSRKb*; Iwano et al., 2015) was crossed to the *atg7-9* mutant (C24 accession; see below). All transgenic lines were genotyped using primers found in Supplemental Table 1. For the C24 accession, plants were genotyped for $AlSCR_b$, $AlSRK_b$ and *atg7-9*. Progeny were analyzed in the F_2 generation for both crosses.

Plasmid construction and plant transformation

The *atg7-9* CRISPR/Cas9 deletion mutation was generated in C24 using previously described methods in the Col-0 accession (Doucet et al., 2019; Doucet et al., 2019). The final pBEE401E vector contained two guide RNAs targeting exons 3 and 8 of *ATG7* (Supplemental Fig. S1). *Arabidopsis thaliana* C24 plants were transformed using floral dip (Clough and Bent, 1998), and plants were dipped twice, 3 days apart, to maximize transformation efficiency. T1 seeds were collected and germinated on soil, and one-week old seedlings were sprayed with BASTA herbicide to select for transformants. PCR was used to confirm transformants (BASTA marker) and the presence of *atg7* mutations (deletions of the exon 3-8 region; Supplemental Figure S1). These *atg7* deletion mutants were then verified through sequencing of regions flanking the deletions. The *atg7* mutants showed a wild-type plant and flower morphology, along with the shorter life span typically seen in *atg* mutants (Thompson et al., 2005; Avila-Ospina et al., 2014). One homozygous mutant, *atg7-9*, from the T2 generation was crossed to the *SI-C24 #15-1* line, and all data was collected in the F_2 generation of this cross (F_4 generation for *atg7-9*). The *GFP-ATG8a* construct (Thompson et al., 2005) was similarly transformed into the C24 accession and crossed to the *SI-C24 #15-1* line.

Confocal Microscopy

A. thaliana SI-C24 plants carrying the *GFP-ATG8a* construct were manually pollinated using pollen from the self-incompatible SI-C24 line. Pistils were removed at 5-min post-pollination, and images of autophagosomes was completed at 10-min post-pollination. All images were taken using a Leica TCS SP8 confocal microscope, with standard GFP excitation-emission wavelengths (488nm excitation, 500-535nm emission). Leica LAS AF lite software was used for all subsequent image processing.

Assays for Pollen hydration, Aniline blue staining, and Seed set

All post-pollination assays used manual pollinations and were conducted as described in (Lee et al., 2020). For the SI-C24 plants, late stage 12 pistils were first emasculated and wrapped in plastic wrap overnight prior to pollination. For the SI-Col-0 plants, the pistils did not require emasculation due to the approach herkogamy phenotype (Zhang et al. 2019*)*, and freshly opened flowers with unpollinated pistils were selected for these assays. All pollinations were completed at humidity levels under 50% for consistency. Pollen hydration assays were conducted by removing and mounting pistils on ½ MS, and lightly pollinating the stigmatic surface using a single anther. Images were taken at 0- and 10-min post-pollination using a Nikon sMz800 microscope, and pollen grains on the stigmatic surface were randomly selected for measurements using the NIS-elements imaging software. For the aniline blue staining, one anther was used to lightly pollinate each pistil, and the pistils were then collected at 2- and 24-hours post-pollination for staining as described in (Lee et al., 2020). The aniline blue-stained pistils were mounted on a slide with sterile water, flattened, and imaged using a Zeiss Axioscope2 Plus fluorescent microscope. For seeds counts, pistils were manually pollinated with a single anther and were left for 10-14 days. The maturing siliques were then removed and cleared in 70% (v/v) ethanol for 3-5 days, or until seeds were visible (Beuder et al., 2020). Siliques were then mounted on a dry slide with the septum facing upwards and imaged using a Nikon sMz800 microscope, and seeds were counted using the NIS-elements imaging software.

Supplemental Material

Supplemental Figure S1. Generation of the *ATG7* CRISPR/Cas9 deletion mutation in the C24 accession.

Supplemental Figure S2. Representative images of flowering plants for the SI-C24 and *atg7-9* mutant plants in the C24 accession.

Supplemental Figure S3. Representative images of aniline blue-stained pistils at 2 hrs following pollination with SI-Col-0 or Col-0 pollen.

Supplemental Figure S4. Representative images of aniline blue-stained pistils at 2 hrs following pollination with SI-C24 or C24 pollen.

Supplemental Figure S5. Heatmap of the *ATG8-ATG12* conjugation system genes expressed in the Stigmatic Papillae RNA-Seq dataset.

Supplemental Table 1. Primer Sequences.

Acknowledgements

We thank Laura Canales and Arjun Sharma for technical assistance, and members of the Goring lab for critically reading this article. We are very grateful to Seiji Takayama (Nara Institute of Science and Technology; University of Tokyo) for providing the *SI-C24 #15-1* seeds (*A. thaliana* C24), Richard Vierstra (Washington University in St Louis) and Peter Bozhkov (Swedish University of Agricultural Sciences) for providing *atg7-2* mutant seeds (*A. thaliana* Col-0), and Richard Vierstra for providing the *GFP:ATG8a* transformation vector.

Figure 1. Pollen hydration assays on control and SI F_2 progeny segregating for the *atg7* mutation.

Pollen hydration assays for **A,** SI-Col-0 pollen grains placed on stigmas from Col-0, SI-Col-0, *atg7-2*, and F_2 progeny from the SI-Col-0 x *atg7-2/atg7-2* cross; and **B,** SI-C24 pollen grains placed on stigmas from C24, SI-C24, *atg7-9*, and F_2 progeny stigmas from the SI-C24 x *atg7-9/atg7-9* cross. Pollen hydration was measured by taking pollen grain diameters at 0- and 10-minutes post-pollination. Data are plotted as box plots displaying first (Q1) and third (Q3) quartiles split by the median; the whiskers extend maximum of 1.5 times the interquartile range beyond the box. Outliers are indicated as black dots. n=30 pollen grains per line, $P<0.05$ (One-way ANOVA with Tukey-HSD post-hoc test).

Figure 2. Representative images of aniline blue-stained pistils at 24 hrs following pollination with SI-Col-0 or Col-0 pollen.

A-G, All stigmas were hand-pollinated with SI-Col-0 pollen or wild-type Col-0 pollen as indicated and collected at 24 hours post-pollination for aniline blue staining. The genotypes of the pistils are indicated for each panel. Pollen tubes penetrating through the stigma and style indicate a breakdown of self-incompatibility as seen in **G**. For each panel, top image = brightfield, bottom image = aniline blue. Scale bar = 100µm

H, Bar graph showing the mean number of pollen tubes at 24 hrs post-pollination. Whiskers represent SE. n = 11-12 pistils per line. At 24 hours, pistils from SI-Col-0 *atg7-2/atg7-2* mutants allowed a significantly higher number of SI-Col-0 pollen tubes compared to the SI-Col-0 pistils ($P<0.05$, One-way ANOVA).

Figure 3. Representative images of aniline blue-stained pistils at 24 hrs following pollination with SI-C24 or C24 pollen.

A-G, All stigmas were hand-pollinated with SI-C24 pollen or wild-type C24 pollen as indicated and collected at 24 hours post-pollination for aniline blue staining. The genotypes of the pistils are indicated for each panel. Pollen tubes penetrating through the stigma and style indicate a breakdown of self-incompatibility as seen in G. For each panel, top image = brightfield, bottom image = aniline blue. Scale bar = 100µm

H, Bar graph showing the mean number of pollen tubes at 24 hrs post-pollination. Whiskers represent SE. n = 8-10 pistils per line. At 24 hours, pistils from SI-C24 *atg7-9/atg7-9* mutants allowed a significantly higher number of SI-C24 pollen tubes compared to the SI-C24 pistils ($P<0.05$, One-way ANOVA).

Figure 4. Seeds per silique counts for control and SI F_2 progeny with the *atg7* mutation.

Seeds per silique counts following manual pollination with **A,** SI-Col-0 pollen or **B,** SI-C24 pollen on pistils with the indicated genotypes. Siliques were harvested at 2-weeks post-pollination and cleared for seeds counts. Compared to the control SI pollinations, significant increases in the number of seeds per silique were observed for the SI-F_2 plants that were either heterozygous or homozygous for the *atg7* mutation. n= 8-10 siliques per line, $P<0.05$ (One-way ANOVA with Tukey-HSD post-hoc test). Data are plotted as box plots displaying first (Q1) and third (Q3) quartiles split by the median; the whiskers extend maximum of 1.5 times the interquartile range beyond the box. Outliers are indicated as black dots.

C-D, Representative images of cleared siliques used in seed counting. Scale bar = 2 mm.

Figure 5. Autophagosomes are visible in SI-C24 papillae when pollinated with SI-C24 pollen.

At 10-minutes post-pollination, several autophagosomes marked by the GFP-ATG8a marker are visible in the SI-C24 stigmatic papillae when pollinated with **A-C,** SI-C24 pollen, but not with **D-E,** wild-type C24 pollen. Scale bar = 10µm

492

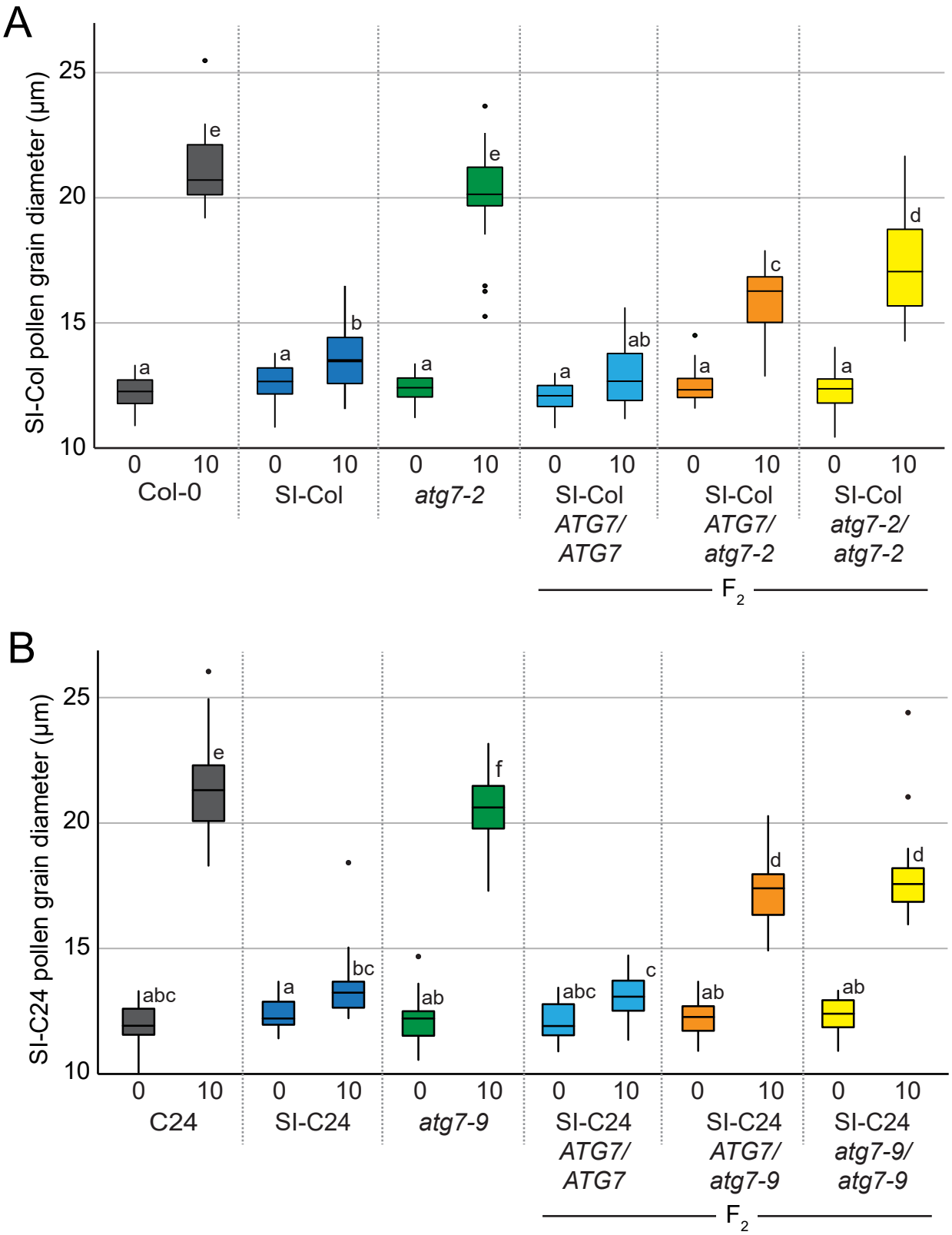

Figure 1. Pollen hydration assays on control and SI F2 progeny segregating for the *atg7* mutation.

Pollen hydration assays for **A,** SI-Col-0 pollen grains placed on stigmas from Col-0, SI-Col-0, *atg7-2*, and F2 progeny from the SI-Col-0 x *atg7-2/atg7-2* cross; and **B,** SI-C24 pollen grains placed on stigmas from C24, SI-C24, *atg7-9*, and F2 progeny stigmas from the SI-C24 x *atg7-9/atg7-9* cross. Pollen hydration was measured by taking pollen grain diameters at 0- and 10-minutes post-pollination. Data are plotted as box plots displaying first (Q1) and third (Q3) quartiles split by the median; the whiskers extend maximum of 1.5 times the interquartile range beyond the box. Outliers are indicated as black dots. n=30 pollen grains per line, $P<0.05$ (One-way ANOVA with Tukey-HSD post-hoc test).

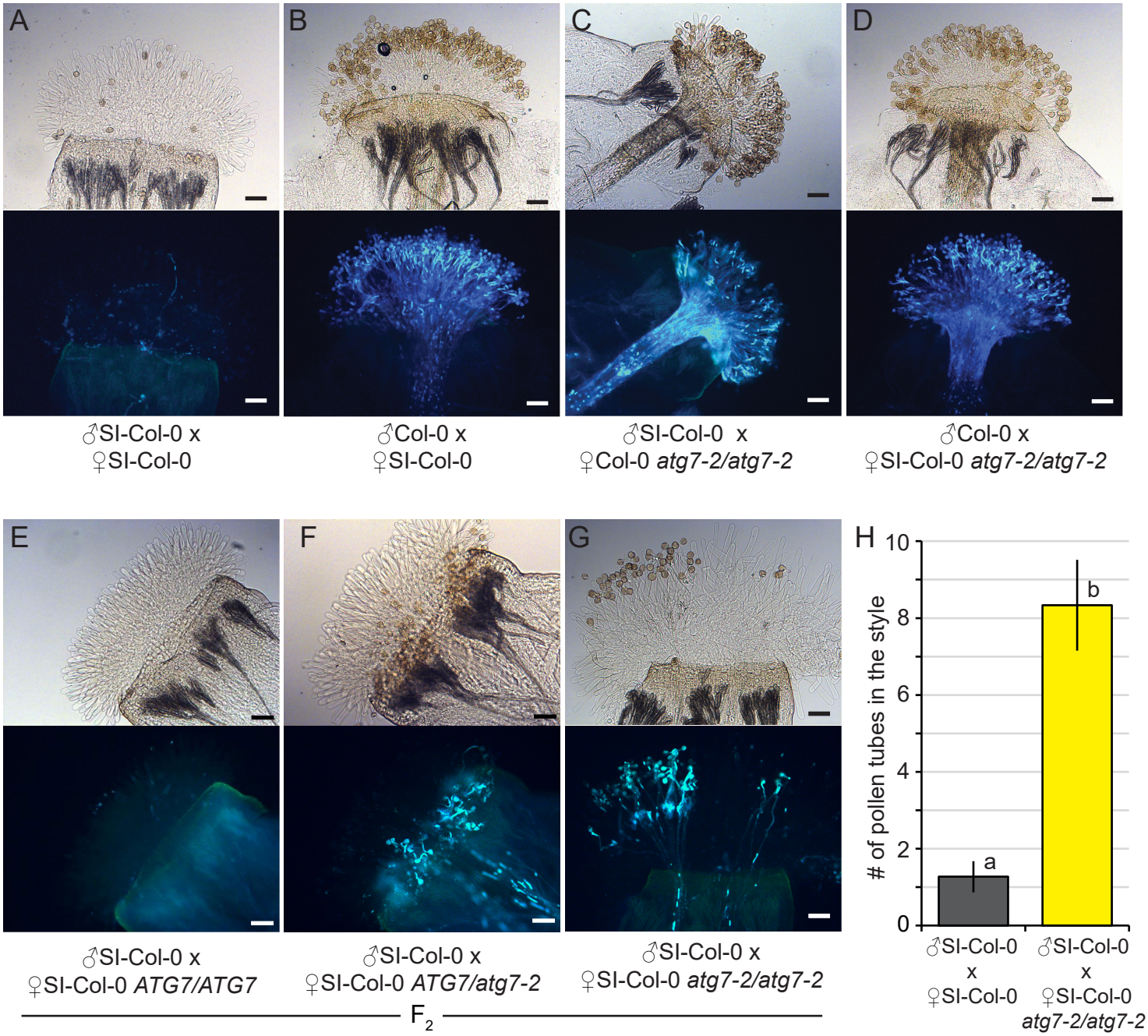

Figure 2. Representative images of aniline blue-stained pistils at 24 hrs following pollination with SI-Col-0 or Col-0 pollen.

A-G, All stigmas were hand-pollinated with SI-Col-0 pollen or wild-type Col-0 pollen as indicated and collected at 24 hours post-pollination for aniline blue staining. The genotypes of the pistils are indicated for each panel. Pollen tubes penetrating through the stigma and style indicate a breakdown of self-incompatibility as seen in G. For each panel, top image = brightfield, bottom image = aniline blue. Scale bar = 100μm

H, Bar graph showing the mean number of pollen tubes at 24 hrs post-pollination. Whiskers represent SE. n = 11-12 pistils per line. At 24 hours, pistils from SI-Col-0 *atg7-2/atg7-2* mutants allowed a significantly higher number of SI-Col-0 pollen tubes compared to the SI-Col-0 pistils ($P<0.05$, One-way ANOVA).

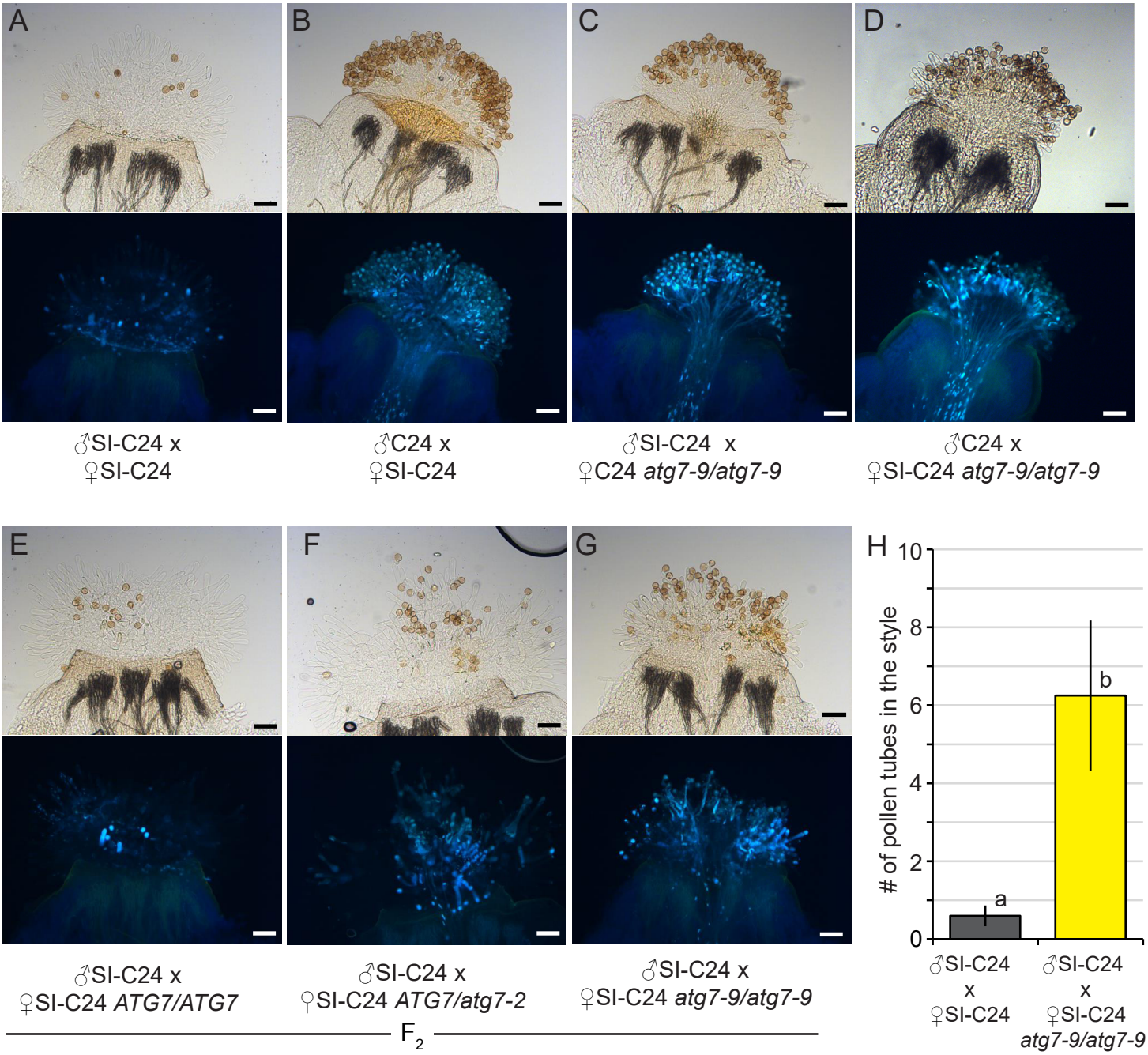

Figure 3. Representative images of aniline blue-stained pistils at 24 hrs following pollination with SI-C24 or C24 pollen.

A-G, All stigmas were hand-pollinated with SI-C24 pollen or wild-type C24 pollen as indicated and collected at 24 hours post-pollination for aniline blue staining. The genotypes of the pistils are indicated for each panel. Pollen tubes penetrating through the stigma and style indicate a breakdown of self-incompatibility as seen in G. For each panel, top image = brightfield, bottom image = aniline blue. Scale bar = 100µm

H, Bar graph showing the mean number of pollen tubes at 24 hrs post-pollination. Whiskers represent SE. n = 8-10 pistils per line. At 24 hours, pistils from SI-C24 *atg7-9/atg7-9* mutants allowed a significantly higher number of SI-C24 pollen tubes compared to the SI-C24 pistils ($P<0.05$, One-way ANOVA).

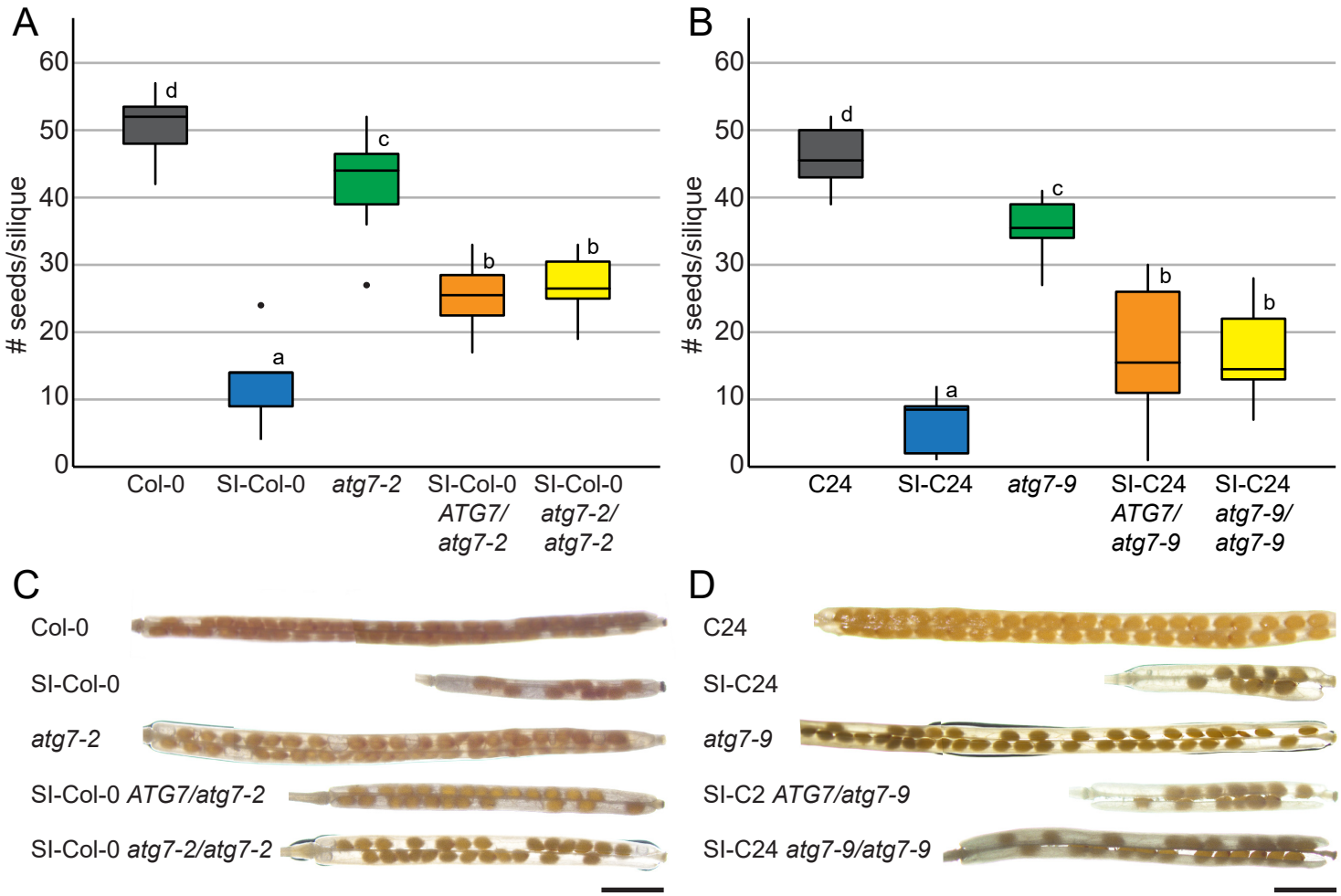

Figure 4. Seeds per silique counts for control and SI F2 progeny with the *atg7* mutation. Seeds per silique counts following manual pollination with **A,** SI-Col-0 pollen or **B,** SI-C24 pollen on pistils with the indicated genotypes. Siliques were harvested at 2-weeks post-pollination and cleared for seeds counts. Compared to the control SI pollinations, significant increases in the number of seeds per silique were observed for the SI-F2 plants that were either heterozygous or homozygous for the *atg7* mutation. n= 8-10 siliques per line, $P<0.05$ (One-way ANOVA with Tukey-HSD post-hoc test). Data are plotted as box plots displaying first (Q1) and third (Q3) quartiles split by the median; the whiskers extend maximum of 1.5 times the interquartile range beyond the box. Outliers are indicated as black dots.
C-D, Representative images of cleared siliques used in seed counting. Scale bar = 2 mm.

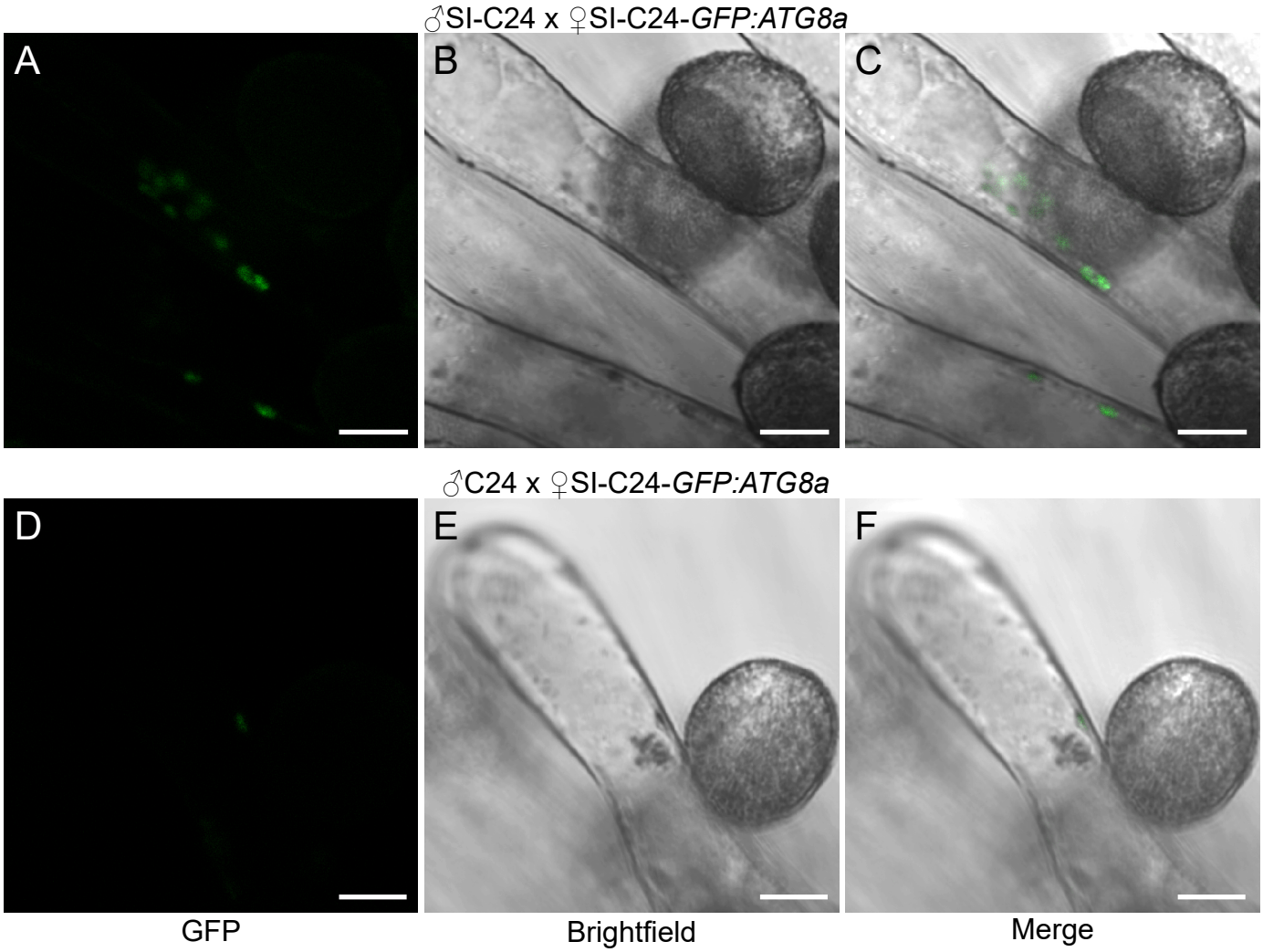

Figure 5. Autophagosomes are visible in SI-C24 papillae when pollinated with SI-C24 pollen.
At 10-minutes post-pollination, several autophagosomes marked by the GFP-ATG8a marker are visible in the SI-C24 stigmatic papillae when pollinated with **A-C,** SI-C24 pollen, but not with **D-E,** wild-type C24 pollen. Scale bar = 10μm

Parsed Citations

Adhikari PB, Liu X, Wu X, Zhu S, Kasahara RD (2020) Fertilization in flowering plants: an odyssey of sperm cell delivery. Plant Mol Biol 103: 9-32
Pubmed: Author and Title
Google Scholar: Author Only Title Only Author and Title

Avila-Ospina L, Moison M, Yoshimoto K, Masclaux-Daubresse C (2014) Autophagy, plant senescence, and nutrient recycling. J Exp Bot 65: 3799-3811
Pubmed: Author and Title
Google Scholar: Author Only Title Only Author and Title

Beuder S, Dorchak A, Bhide A, Moeller SR, Petersen BL, MacAlister CA (2020) Exocyst mutants suppress pollen tube growth and cell wall structural defects of hydroxyproline O-arabinosyltransferase mutants. Plant J 103: 1399-1419
Pubmed: Author and Title
Google Scholar: Author Only Title Only Author and Title

Boggs NA, Nasrallah JB, Nasrallah ME (2009) Independent S-Locus Mutations Caused Self-Fertility in Arabidopsis thaliana. Plos Genetics 5: e1000426.
Pubmed: Author and Title
Google Scholar: Author Only Title Only Author and Title

Chung T, Phillips AR, Vierstra RD (2010) ATG8 lipidation and ATG8-mediated autophagy in Arabidopsis require ATG12 expressed from the differentially controlled ATG12A AND ATG12B loci. Plant J 62: 483-493
Pubmed: Author and Title
Google Scholar: Author Only Title Only Author and Title

Clough SJ, Bent AF (1998) Floral dip: A simplified method for Agrobacterium-mediated transformation of Arabidopsis thaliana. Plant J 16: 735-743
Pubmed: Author and Title
Google Scholar: Author Only Title Only Author and Title

Dickinson H (1995) Dry stigmas, water and self-incompatibility in Brassica. Sex Plant Reprod 8: 1-10
Pubmed: Author and Title
Google Scholar: Author Only Title Only Author and Title

Ding X, Zhang X, Otegui MS (2018) Plant autophagy: new flavors on the menu. Curr Opin Plant Biol 46: 113-121
Pubmed: Author and Title
Google Scholar: Author Only Title Only Author and Title

Doucet J, Lee HK, Goring DR (2016) Pollen acceptance or rejection: a tale of two pathways. Trends Plant Sci 21: 1058-1067
Pubmed: Author and Title
Google Scholar: Author Only Title Only Author and Title

Doucet J, Lee HK, Udugama N, Xu J, Qi B, Goring DR (2019) Investigations into a putative role for the novel BRASSIKIN pseudokinases in compatible pollen-stigma interactions in Arabidopsis thaliana. BMC Plant Biol 19: 549
Pubmed: Author and Title
Google Scholar: Author Only Title Only Author and Title

Doucet J, Truong C, Frank-Webb E, Lee HK, Daneva A, Gao Z, Nowack MK, Goring DR (2019) Identification of a role for an E6-like 1 gene in early pollen-stigma interactions in Arabidopsis thaliana. Plant Reprod 32: 307-322
Pubmed: Author and Title
Google Scholar: Author Only Title Only Author and Title

Durand E, Chantreau M, Le Veve A, Stetsenko R, Dubin M, Genete M, Llaurens V, Poux C, Roux C, Billiard S, Vekemans X, Castric V (2020) Evolution of self-incompatibility in the Brassicaceae: Lessons from a textbook example of natural selection. Evol Appl 13: 1279-1297
Pubmed: Author and Title
Google Scholar: Author Only Title Only Author and Title

Elleman C, Dickinson H (1996) Identification of pollen of components regulating the responses in stigmatic Brassica oleracea. New Phytol 133: 197-205
Pubmed: Author and Title
Google Scholar: Author Only Title Only Author and Title

Fujii S, Shimosato-Asano H, Kakita M, Kitanishi T, Iwano M, Takayama S (2020) Parallel evolution of dominant pistil-side self-incompatibility suppressors in Arabidopsis. Nat Commun 11: 1404
Pubmed: Author and Title
Google Scholar: Author Only Title Only Author and Title

Gao Z, Daneva A, Salanenka Y, Van Durme M, Huysmans M, Lin ZC, De Winter F, Vanneste S, Karimi M, Van de Velde J, Vandepoele K, Van de Walle D, Dewettinck K, Lambrecht BN, Nowack MK (2018) KIRA1 and ORESARA1 terminate flower receptivity by promoting cell death in the stigma of Arabidopsis. Nat Plants 4:365-375
Pubmed: Author and Title

Google Scholar: Author Only Title Only Author and Title

Goring DR (2017) Exocyst, exosomes, and autophagy in the regulation of Brassicaceae pollen-stigma interactions. J Exp Bot 69: 69-78
Pubmed: Author and Title
Google Scholar: Author Only Title Only Author and Title

Goubet PM, Berges H, Bellec A, Prat E, Helmstetter N, Mangenot S, Gallina S, Holl AC, Fobis-Loisy I, Vekemans X, Castric V (2012) Contrasted patterns of molecular evolution in dominant and recessive self-incompatibility haplotypes in Arabidopsis. PLoS Genet 8: e1002495
Pubmed: Author and Title
Google Scholar: Author Only Title Only Author and Title

Gu T, Mazzurco M, Sulaman W, Matias DD, Goring DR (1998) Binding of an arm repeat protein to the kinase domain of the S-locus receptor kinase. Proc Natl Acad Sci 95: 382-387
Pubmed: Author and Title
Google Scholar: Author Only Title Only Author and Title

Guo YL, Zhao X, Lanz C, Weigel D (2011) Evolution of the S-locus region in Arabidopsis relatives. Plant Physiol 157: 937-946
Pubmed: Author and Title
Google Scholar: Author Only Title Only Author and Title

Indriolo E, Goring DR (2014) A conserved role for the ARC1 E3 ligase in Brassicaceae self-incompatibility. Front Plant Sci 5: 181
Pubmed: Author and Title
Google Scholar: Author Only Title Only Author and Title

Indriolo E, Goring DR (2016) Yeast two-hybrid interactions between Arabidopsis lyrata S Receptor Kinase and the ARC1 E3 ligase. Plant Signal Behav 11: e1188233
Pubmed: Author and Title
Google Scholar: Author Only Title Only Author and Title

Indriolo E, Safavian D, Goring DR (2014) The ARC1 E3 Ligase Promotes Two Different Self-Pollen Avoidance Traits in Arabidopsis. Plant Cell 26: 1525-1543
Pubmed: Author and Title
Google Scholar: Author Only Title Only Author and Title

Indriolo E, Safavian D, Goring DR (2014) The ARC1 E3 ligase promotes two different self-pollen avoidance traits in Arabidopsis. Plant Cell 26: 1525-1543
Pubmed: Author and Title
Google Scholar: Author Only Title Only Author and Title

Indriolo E, Tharmapalan P, Wright SI, Goring DR (2012) The ARC1 E3 ligase gene is frequently deleted in self-compatible Brassicaceae species and has a conserved role in Arabidopsis lyrata self-pollen rejection. Plant Cell 24: 4607-4620
Pubmed: Author and Title
Google Scholar: Author Only Title Only Author and Title

Iwano M, Igarashi M, Tarutani Y, Kaothien-Nakayama P, Nakayama H, Moriyama H, Yakabe R, Entani T, Shimosato-Asano H, Ueki M, Tamiya G, Takayama S (2014) A Pollen Coat–Inducible Autoinhibited Ca2+-ATPase Expressed in Stigmatic Papilla Cells Is Required for Compatible Pollination in the Brassicaceae. Plant Cell 26: 636-649
Pubmed: Author and Title
Google Scholar: Author Only Title Only Author and Title

Iwano M, Ito K, Fujii S, Kakita M, Asano-Shimosato H, Igarashi M, Kaothien-Nakayama P, Entani T, Kanatani A, Takehisa M, Tanaka M, Komatsu K, Shiba H, Nagai T, Miyawaki A, Isogai A, Takayama S (2015) Calcium signalling mediates self-incompatibility response in the Brassicaceae. Nat Plants 1: 15128
Pubmed: Author and Title
Google Scholar: Author Only Title Only Author and Title

Jany E, Nelles H, Goring DR (2019) The Molecular and Cellular Regulation of Brassicaceae Self-Incompatibility and Self-Pollen Rejection, 343: 1-35
Pubmed: Author and Title
Google Scholar: Author Only Title Only Author and Title

Johnson MA, Harper JF, Palanivelu R (2019) A Fruitful Journey: Pollen Tube Navigation from Germination to Fertilization. Annu Rev Plant Biol 70: 809-837
Pubmed: Author and Title
Google Scholar: Author Only Title Only Author and Title

Kusaba M, Dwyer K, Hendershot J, Vrebalov J, Nasrallah JB, Nasrallah ME (2001) Self-Incompatibility in the Genus Arabidopsis: Characterization of the S Locus in the Outcrossing A. Lyrata and Its Autogamous Relative A. thaliana. Plant Cell 13: 627-644
Pubmed: Author and Title
Google Scholar: Author Only Title Only Author and Title

Lee HK, Macgregor S, Goring DR (2020) A Toolkit for Teasing Apart the Early Stages of Pollen-Stigma Interactions in Arabidopsis thaliana. Methods Mol Biol 2160: 13-28
Pubmed: Author and Title

Google Scholar: Author Only Title Only Author and Title

Marshall RS, Vierstra RD (2018) Autophagy: The Master of Bulk and Selective Recycling. Annu Rev Plant Biol 69: 173-208
Pubmed: Author and Title
Google Scholar: Author Only Title Only Author and Title

Minina EA, Moschou PN, Vetukuri RR, Sanchez-Vera V, Cardoso C, Liu Q, Elander PH, Dalman K, Beganovic M, Lindberg Yilmaz J, Marmon S, Shabala L, Suarez MF, Ljung K, Novak O, Shabala S, Stymne S, Hofius D, Bozhkov PV (2018) Transcriptional stimulation of rate-limiting components of the autophagic pathway improves plant fitness. J Exp Bot 69: 1415-1432
Pubmed: Author and Title
Google Scholar: Author Only Title Only Author and Title

Mizuta Y, Higashiyama T (2018) Chemical signaling for pollen tube guidance at a glance. J Cell Sci 131: jcs208447
Pubmed: Author and Title
Google Scholar: Author Only Title Only Author and Title

Nasrallah JB (2019) Self-incompatibility in the Brassicaceae: Regulation and mechanism of self-recognition. Curr Top Dev Biol 131: 435-452
Pubmed: Author and Title
Google Scholar: Author Only Title Only Author and Title

Nasrallah ME, Liu P, Nasrallah JB (2002) Generation of self-incompatible Arabidopsis thaliana by transfer of two S locus genes from A. lyrata. Science 297: 247-249
Pubmed: Author and Title
Google Scholar: Author Only Title Only Author and Title

Nasrallah ME, Liu P, Sherman-Broyles S, Boggs NA, Nasrallah JB (2004) Natural variation in expression of self-incompatibility in Arabidopsis thaliana: Implications for the evolution of selfing. Proc Natl Acad Sci 101: 16070-16074
Pubmed: Author and Title
Google Scholar: Author Only Title Only Author and Title

Palanivelu R, Tsukamoto T (2012) Pathfinding in angiosperm reproduction: pollen tube guidance by pistils ensures successful double fertilization. Wiley Interdiscip Rev Dev Biol 1:96-113
Pubmed: Author and Title
Google Scholar: Author Only Title Only Author and Title

Phillips AR, Suttangkakul A, Vierstra RD (2008) The ATG12-conjugating enzyme ATG10 Is essential for autophagic vesicle formation in Arabidopsis thaliana. Genetics 178: 1339-1353
Pubmed: Author and Title
Google Scholar: Author Only Title Only Author and Title

Qi H, Xia FN, Xiao S (2020) Autophagy in plants: Physiological roles and post-translational regulation. J Integr Plant Biol Apr 23. doi: 10.1111/jipb.12941 Online ahead of print.
Pubmed: Author and Title
Google Scholar: Author Only Title Only Author and Title

Qin G, Ma Z, Zhang L, Xing S, Hou X, Deng J, Liu J, Chen Z, Qu LJ, Gu H (2007) Arabidopsis AtBECLIN 1/AtAtg6/AtVps30 is essential for pollen germination and plant development. Cell Res 17: 249-263
Pubmed: Author and Title
Google Scholar: Author Only Title Only Author and Title

Rodriguez E, Chevalier J, Olsen J, Ansbol J, Kapousidou V, Zuo Z, Svenning S, Loefke C, Koemeda S, Drozdowskyj PS, Jez J, Durnberger G, Kuenzl F, Schutzbier M, Mechtler K, Ebstrup EN, Lolle S, Dagdas Y, Petersen M (2020) Autophagy mediates temporary reprogramming and dedifferentiation in plant somatic cells. EMBO J 39: e103315
Pubmed: Author and Title
Google Scholar: Author Only Title Only Author and Title

Rozier F, Riglet L, Kodera C, Bayle V, Durand E, Schnabel J, Gaude T, Fobis-Loisy I (2020) Live-cell imaging of early events following pollen perception in self-incompatible Arabidopsis thaliana. J Exp Bot 71: 2513-2526.
Pubmed: Author and Title
Google Scholar: Author Only Title Only Author and Title

Safavian D, Goring DR (2013) Secretory activity is rapidly induced in stigmatic papillae by compatible pollen, but inhibited for self-incompatible pollen in the brassicaceae. PLoS ONE 8
Pubmed: Author and Title
Google Scholar: Author Only Title Only Author and Title

Safavian D, Zayed Y, Indriolo E, Chapman L, Ahmed A, Goring DR (2015) RNA silencing of exocyst genes in the stigma impairs the acceptance of compatible pollen in Arabidopsis. Plant Physiol 169: 2526-2538
Pubmed: Author and Title
Google Scholar: Author Only Title Only Author and Title

Samuel MA, Chong YT, Haasen KE, Aldea-Brydges MG, Stone SL, Goring DR (2009) Cellular Pathways Regulating Responses to Compatible and Self-Incompatible Pollen in Brassicaand ArabidopsisStigmas Intersect at Exo70A1, a Putative Component of the Exocyst Complex. Plant Cell 21: 2655-2671

Pubmed: Author and Title
Google Scholar: Author Only Title Only Author and Title

Samuel MA, Chong YT, Haasen KE, Aldea-Brydges MG, Stone SL, Goring DR (2009) Cellular pathways regulating responses to compatible and self-incompatible pollen in Brassica and Arabidopsis stigmas intersect at Exo70A1, a putative component of the exocyst complex. Plant Cell 21: 2655-2671
Pubmed: Author and Title
Google Scholar: Author Only Title Only Author and Title

Sankaranarayanan S, Jamshed M, Samuel MA (2015) Degradation of glyoxalase I in Brassica napus stigma leads to self-incompatibility response. Nat Plants 1: 1-7
Pubmed: Author and Title
Google Scholar: Author Only Title Only Author and Title

Sankaranarayanan S, Jamshed M, Samuel MA (2015) Degradation of glyoxalase I in Brassica napus stigma leads to self-incompatibility response. Nat Plants 1: 15185
Pubmed: Author and Title
Google Scholar: Author Only Title Only Author and Title

Schierup MH, Mable BK, Awadalla P, Charlesworth D (2001) Identification and characterization of a polymorphic receptor kinase gene linked to the self-incompatibility locus of Arabidopsis lyrata. Genetics 158: 387-399
Pubmed: Author and Title
Google Scholar: Author Only Title Only Author and Title

Shimizu KK, Shimizu-Inatsugi R, Tsuchimatsu T, Purugganan MD (2008) Independent origins of self-compatibility in Arabidopsis thaliana. Mol Ecol 17: 704-714
Pubmed: Author and Title
Google Scholar: Author Only Title Only Author and Title

Shimizu KK, Tsuchimatsu T (2015) Evolution of Selfing: Recurrent Patterns in Molecular Adaptation. Annu Rev Ecol Evol Syst 46: 593-622
Pubmed: Author and Title
Google Scholar: Author Only Title Only Author and Title

Stone SL, Anderson EM, Mullen RT, Goring DR (2003) ARC1 is an E3 ubiquitin ligase and promotes the ubiquitination of proteins during the rejection of self-incompatible Brassica pollen. Plant Cell 15: 885-898
Pubmed: Author and Title
Google Scholar: Author Only Title Only Author and Title

Stone SL, Arnoldo M, Goring DR (1999) A breakdown of Brassica self-incompatibility in ARC1 antisense transgenic plants. Science 286: 1729-1731
Pubmed: Author and Title
Google Scholar: Author Only Title Only Author and Title

Su T, Li X, Yang M, Shao Q, Zhao Y, Ma C, Wang P (2020) Autophagy: An Intracellular Degradation Pathway Regulating Plant Survival and Stress Response. Front Plant Sci 11: 164
Pubmed: Author and Title
Google Scholar: Author Only Title Only Author and Title

Thompson AR, Doelling JH, Suttangkakul A, Vierstra RD (2005) Autophagic nutrient recycling in Arabidopsis directed by the ATG8 and ATG12 conjugation pathways. Plant Physiol 138: 2097-2110
Pubmed: Author and Title
Google Scholar: Author Only Title Only Author and Title

Tsuchimatsu T, Goubet PM, Gallina S, Holl AC, Fobis-Loisy I, Berges H, Marande W, Prat E, Meng D, Long Q, Platzer A, Nordborg M, Vekemans X, Castric V (2017) Patterns of Polymorphism at the Self-Incompatibility Locus in 1,083 Arabidopsis thaliana Genomes. Mol Biol Evol 34: 1878-1889
Pubmed: Author and Title
Google Scholar: Author Only Title Only Author and Title

Tsuchimatsu T, Suwabe K, Shimizu-Inatsugi R, Isokawa S, Pavlidis P, Stadler T, Suzuki G, Takayama S, Watanabe M, Shimizu KK (2010) Evolution of self-compatibility in Arabidopsis by a mutation in the male specificity gene. Nature 464: 1342-1346
Pubmed: Author and Title
Google Scholar: Author Only Title Only Author and Title

Young PG, Passalacqua MJ, Chappell K, Llinas RJ, Bartel B (2019) A facile forward-genetic screen for Arabidopsis autophagy mutants reveals twenty-one loss-of-function mutations disrupting six ATG genes. Autophagy 15: 941-959
Pubmed: Author and Title
Google Scholar: Author Only Title Only Author and Title

Zhang T, Zhou G, Goring DR, Liang X, Macgregor S, Dai C, Wen J, Yi B, Shen J, Tu J, Fu T, Ma C (2019) Generation of Transgenic Self-Incompatible Arabidopsis thaliana Shows a Genus-Specific Preference for Self-Incompatibility Genes. Plants (Basel) 8: 570
Pubmed: Author and Title
Google Scholar: Author Only Title Only Author and Title